Shape Optimization for the Submerged Body of a Two-Body Wave Energy Converter

Dillon Martin[#1], Adam Wise[#2], Changwei Laing[*#3], and Lei Zuo[#4]

[#]*Department of Mechanical Engineering, Virginia Tech*
Blacksburg, VA 24061, USA

[1]dilmart@vt.edu

[2]adamwise@vt.edu

[4]leizuo@vt.edu

[*]*Department of Mechanical Engineering, Stony Brook University*
Stony Brook, NY 11794, USA

[3]changwei.liang@stonybrook.edu

***Abstract*— The shape of the submerged body on a two-body wave energy converter is studied in this paper. For this study, varying shapes and sizes of the submerged body are investigated to see the influence the submerged body has on the absorption power of a two-body system. Three different submerged body shapes are investigated; plate, cylinder and sphere. The hydrodynamic parameters for the varying shapes and sizes of the submerged body are calculated using boundary element method software (WAMIT). The two-body dynamics are modelled in WEC-Sim. Simulations were completed for both regular and irregular wave conditions. It is found that the maximum power for each shape will occur at a certain mass ratio. It is also found that for small to no viscous effects, the power of the two-body system can exceed that of a single body system. Small viscous effects however become unrealistic with increasing submerged body size. Simulations show the cylinder performing the best, the sphere performing slightly worse than the cylinder, and the plate performing the worst.**

***Keywords*— wave energy conversion; two-body point absorber; shape optimization; mass ratio; drag**

I. Introduction

One method of developing a resonant wave energy converter (WEC) is a two-body point absorber. The two-body WEC uses the relative motion between a floating buoy and a submerged body to capture energy. Advantages of a two-body WEC include easier ocean implementation (mooring, generator instalment, etc.) and dynamic performance (parameter optimization). Different two body devices use different submerged body designs however. Reference Model 3 (RM3), sponsored by the U.S. Department of Energy (DOE) to benchmark marine hydrokinetic technology performance and costs, uses a heave plate to maintain a relatively stationary position [1]. This design is advantageous for easy ocean implementation; however, it is designed to keep the submerged body stationary, meaning its maximum capable power is that of a single-body WEC. Other designs, such as the Wavebob, use a streamlined submerged body to achieve a greater relative velocity between the two bodies [2].

Beatty et al. [3] conducted experimental and numerical comparisons of two self-reacting point absorbers, modelled after the Wavebob [2] and PowerBuoy [4], which was the inspiration for the RM3 device [1]. Their experimental results for added mass and excitation force matched very well with the numerical BEM simulations, however the total damping coefficients were much larger in the experiment. The damping component found for the heave plate design (PowerBuoy) was significantly larger than that of the streamlined design (Wavebob), indicating that viscosity plays a significant role in the submerged body design. After applying viscous damping to their numerical model, their heave RAOs were able to match the experimental RAOs very well.

Further, a study by Liang [5] found that power could be optimized through the mass ratio of the submerged body and flouting buoy. Using linear wave theory and incorporating a linear viscous drag force into the two-body dynamics, Liang found closed-form solutions for both an optimal (using both a restoring spring and damper) and suboptimal (using only a damper) power takeoff (PTO) design. While [5] found that the optimal design performed better in regular waves, the suboptimal design performed slightly better in irregular waves. In this paper, only the suboptimal design is considered.

A simple way to achieve an optimal mass ratio is to manipulate the submerged body's added mass, which can be achieved by increasing its cross sectional area. However, viscous force is proportional to cross section area. The other method would be to increase the dry mass of the submerged body, however one has to take into consideration the buoyancy of the overall system. For this study, varying shapes and sizes of the submerged body, with neutrally buoyant properties, are investigated to see the influence the submerged body has on the absorption power of a two-body system. Three shapes are considered (plate, cylinder and sphere) with varying sizes to achieve similar mass ratios.

II. Dynamic Analysis of a Two-Body Wave Energy Converter

The two-body wave energy converter, shown in Fig. 1, consists of two axisymmetric masses, a floating buoy and a submerged body, subjected to an incident wave. The floating buoy and submerged body are connected through a linear

power takeoff device (PTO). Energy is extracted from the relative motion of both masses. The hydrodynamic parameters are calculated using linear wave theory. For this system, it is assumed that the submerged body is far enough away from the top buoy that the hydrodynamically coupled radiation terms are negligible. As well, for a realistic system, additional viscous forces are included by means of a loss resistance [6].

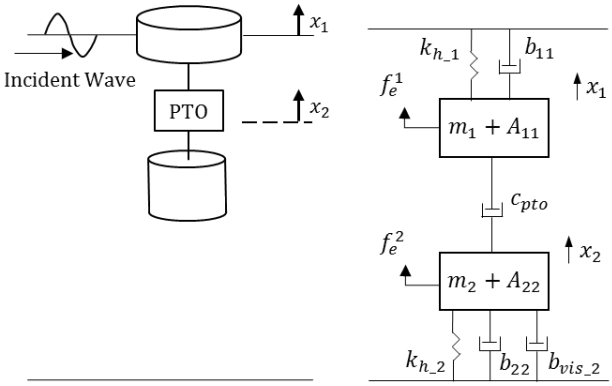

Fig. 1 Schematic and equivalent dynamic model of a two-body wave energy converter

The simplified equations of motion of the two-body system oscillating in heave are:

$$(m_1 + A_{11})\ddot{x}_1 + (c_{PTO} + b_{11})\dot{x}_1 + k_{h\_1}x_1 - c_{PTO}\dot{x}_2 = f_{e\_1} \quad (1)$$

$$(m_2 + A_{22})\ddot{x}_2 + (c_{PTO} + b_{22} + b_{vis\_2})\dot{x}_2 + k_{h\_2}x_2 - c_{PTO}\dot{x}_1 = f_{e\_2} \quad (2)$$

where x_1 and x_2 are the heave displacements of the floating buoy and submerged body, m_1 and m_2 are the masses of the floating buoy and submerged body, Aij and b_{ij} ($i, j = 1, 2$) are the frequency dependent added mass and radiation damping coefficients of the i-th body induced by the motion of the j-th body (1 and 2 represent the floating buoy and submerged body, respectively), k_{h_1} and k_{h_2} are the hydrostatic stiffness's of the floating buoy and submerged body, f_{e_1} and f_{e_2} are frequency dependent excitation forces on the floating buoy and submerged body, and c_{pto} is the damping coefficient for the PTO. Reference [5] shows that power can be optimized through the mass ratio of the submerged body and floating buoy. Closed-form solutions for both an optimal (using both a restoring spring and damper) and a suboptimal (using only a damper) PTO design exist. In regular wave analysis, the optimal design performed the best, as it can always achieve a damped natural frequency that matches the wave excitation frequency. However, in irregular wave analysis, the suboptimal design performed slightly better, which is why c_{pto} is only considered in our model. A viscous damping coefficient for the submerged body, b_{vis_2}, is added to the dynamic model for practicality. From [4], experimental data shows that damping on the top buoy is dominated by the radiation damping and drag has minimal effects, thus it is left off of our dynamic model.

Under regular wave excitation, the exciting force can be expressed as the following harmonic function:

$$f_{e\_1}(t) = F_1 e^{j\omega t},\ f_{e\_2}(t) = F_2 e^{j\omega t} \quad (3), (4)$$

Using the method of undetermined coefficients, we assume that the particular solution takes the same form as the forcing function. That is:

$$x_1(t) = X_1 e^{j\omega t},\ x_2(t) = X_2 e^{j\omega t} \quad (5), (6)$$

Plugging Eqs. 3 – 6 into Eqs. 1 and 2 results in the frequency domain equations of motion, which can be written in matrix form as:

$$\left(-\omega^2 \boldsymbol{M} + j\omega \boldsymbol{C} + \boldsymbol{K}\right)\boldsymbol{X} = \boldsymbol{F} \quad (7)$$

where:

$$\boldsymbol{M} = \begin{bmatrix} m_1 + A_{11} & 0 \\ 0 & m_2 + A_{22} \end{bmatrix} \boldsymbol{C} = \begin{bmatrix} c_{pto} + b_{11} & -c_{pto} \\ -c_{pto} & c_{pto} + b_{22} + b_{vis\_2} \end{bmatrix}$$

$$\boldsymbol{K} = \begin{bmatrix} k_{h\_1} & 0 \\ 0 & k_{h\_2} \end{bmatrix} \boldsymbol{X} = \begin{bmatrix} X_1 \\ X_2 \end{bmatrix} \boldsymbol{F} = \begin{bmatrix} F_1 \\ F_2 \end{bmatrix}$$

A linear PTO is assumed in this model, and the power extracted is from the relative motion of the two bodies:

$$P = c_{PTO}\left|\dot{x}_1 - \dot{x}_2\right|^2 = \frac{1}{2}\omega^2 c_{PTO}\left|X_1 - X_2\right|^2 \quad (8)$$

To maximize the power, we want to maximize the amplitude of displacement, which occurs at resonance. To achieve resonance, the damped natural frequency must match the regular wave excitation frequency. To calculate the natural frequencies and damped natural frequencies, the complex eigenvalues can be solved by setting the determinant of Eq. 7 to zero. The solution will result in two complex conjugate pole pairs, of which the complex magnitudes correspond to the two natural frequencies, and the imaginary terms correspond to the two damped natural frequencies.

As shown in [5], the damped natural frequencies of this system decrease with increasing submerged body mass.

Typical wave periods from a field station offshore the port of Keelung (nearby National Taiwan Ocean University), which will be our experimental test site in the future, are 6 – 10 s [7]. For a single-body design, to achieve natural frequencies similar to the wave excitation frequencies (0.63 – 1.05 rad/s), the total mass (dry mass and added mass) must be the same order of magnitude as the hydrostatic stiffness. It is difficult to achieve a natural frequency similar to the wave frequency by way of the top buoy design, as to increase mass, the volume must also increase to maintain positive buoyancy. It is much simpler to design a submerged body to achieve a damped natural frequency similar to the wave frequency.

While the top buoy design can be optimized to produce a wider bandwidth for wave energy conversion, this paper focuses solely on the submerged body design and its effect on matching the damped natural frequency with the wave excitation frequency. The top buoy and PTO column remain the same sizes for each submerged body design.

III. Submerged Body Design

The optimal mass ratio of the WEC can be achieved through the hydrodynamic added mass and the dry mass of the submerged body. This study examines three submerged body

shapes; a plate, a cylinder and a sphere. The plate will achieve an optimal mass ratio through its added mass by increasing the diameter while maintaining a constant thickness. The cylinder will achieve an optimal mass ratio through its dry mass by increasing the height while maintaining a constant diameter. The sphere will achieve an optimal mass ratio through both added mass and dry mass by increasing the diameter. Fig. 2 shows the configurations of the three WECs.

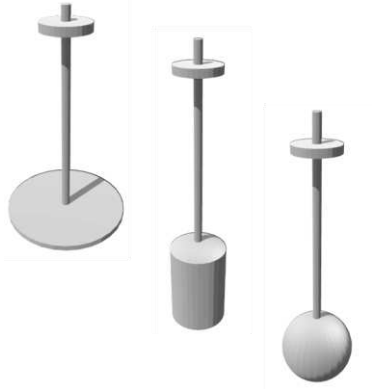

Fig. 2 Configurations of the point absorber using three different submerged body shapes; a plate, a cylinder and a sphere. The top buoy is the same for all three configurations.

Table 1 shows the sizes that were simulated in the time domain for each shape and configuration.

TABLE I
SHAPE SIZES FOR TIME DOMAIN SIMULATIONS

Plate		Cylinder		Sphere	
Diameter (in.)	Mass Ratio	Height (in.)	Mass Ratio	Diameter (in.)	Mass Ratio
60	7	30	12	45	5
75	12	60	18	60	11
90	20	90	24	75	22
95	23	105	26	80	26
100	27	120	29	85	31
105	31	135	32	87.5	34
110	36	150	35	90	37
111	37	165	37	92.5	40
115	41	180	40	95	44
120	46	200	44	100	51
125	51	220	48	105	59
135	64	260	55	120	88
180	146	400	81	200	405

IV. TIME DOMAIN SIMULATIONS

Time domain simulations were completed using the open-source simulation tool, WEC-Sim [8]. WEC-Sim is a code developed by Sandia National Laboratories and the National Renewable Energy Laboratory to model WECs subjected to operational waves in the time domain. WEC-Sim was developed in MATLAB/Simulink to solve the WECs governing equations using the Cummins time-domain impulse response function formulation in 6DOF (12DOF for two-bodies) [9]. In this study, we constrained the system to 2DOF, constraining the overall system in heave, and allowing translation between the two bodies. The convolution integral calculation, based on the Cummins equation, is used to include the memory effect on the system. The radiation force, which were previously determined as Aij and b_{ij} (i, j = 1, 2), can be calculated by:

$$F_{rad} = -A_{\infty}\ddot{x} - \int_0^t K(t-\tau)\dot{x}(\tau)d\tau \tag{9}$$

where A_{∞} is the infinite frequency added mass and K is the radiation impulse response function. WEC-Sim models drag using the quadratic damping force:

$$F_v = C_d \rho A_D (\dot{x}_1 - \dot{x}_2)|\dot{x}_1 - \dot{x}_2| \tag{10}$$

where C_d is the coefficient of drag, ρ is the fluid density, and A_D is the characteristic area [8]. This is a more accurate version of the viscous damping coefficient, b_{vis_2}, that was used in [5] and [6] to find a closed form solution.

Eqs. 1 and 2 can be re-written in the time-domain as:

$$(m_1 + A_{\infty 1})\ddot{x}_1 + c_{PTO}\dot{x}_1 + \int_0^t K_1(t-\tau)\dot{x}_1(\tau)d\tau + k_{h\_1}x_1 - c_{PTO}\dot{x}_2 = f_{e\_1} \tag{11}$$

$$(m_2 + A_{\infty 2})\ddot{x}_2 + (c_{PTO} + b_{vis\_2})\dot{x}_2 + \int_0^t K_2(t-\tau)\dot{x}_2(\tau)d\tau + k_{h\_2}x_2 - c_{PTO}\dot{x}_1 = f_{e\_2} \tag{12}$$

The frequency dependent hydrodynamic parameters used in WEC-Sim are calculated using the commercial BEM software, WAMIT [8]. Simulations were run for both regular and irregular waves. All simulations were run using a water depth of 30m.

V. REGULAR WAVES RESULTS

In this section, the simulation results of the two-body WEC are presented under regular wave excitation using a wave period and wave height of 6s and 1.5m, respectively. The system parameters for the two-body WEC are shown in Fig. 3. Varying sizes, shown in Table 1, for each submerged body shape were analyzed to achieve a wide range of mass ratios. While the size of each shape changes, the distance between the top buoy and the submerged body remained a constant 200in (5.1m). The top buoy remained the same size for each simulation as well. Figures 4 – 6 show the average power vs. mass ratio results for the plate, cylinder and sphere, respectively. Here, the mass ratio is defined as the total mass of the submerged body ($M_2 = m_2 + A_{22}$), divided by the dry mass of the top buoy (m_1). Due to unrealistic WEC motion (close to exceeding the water depth) around resonance, as well as for clarity of other simulation data, the average power is limited to 5 kW.

When there is no drag damping on the submerged body ($C_d = 0$), all three shapes have similar profiles. They each reach resonance conditions at a mass ratio of approximately 35. The

power at that mass ratio exceeds the maximum power of a single body WEC (using the same top buoy as the two-body WEC). As the mass ratio increases past resonance, the power decreases below the maximum power of the single body WEC and becomes steady. As the submerged bodies mass increases, its motion converges to the surrounding particle velocity, which is why the power does not converge to the maximum power of the single body WEC.

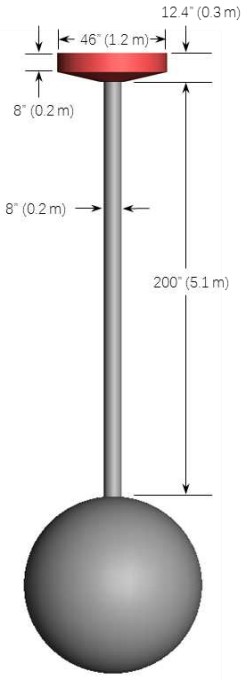

Fig. 3 Overall two-body WEC design with a spherical submerged body

Without experimental results, it is difficult to determine an accurate drag coefficient. Therefore, various drag coefficients ($C_d = 0.5,\ 1\ \&\ 2$) were selected to investigate the effect of the drag coefficient on the system response and power absorption.

Adding drag damping to the submerged body decreases the power significantly. The average power of the plate design, Fig. 4, does not exceed the single body maximum power for any of the drag cases. From Eq. 10, not only does the drag coefficient increase the viscous drag force, the characteristic area increases it as well. As the size of the plate increases, the drag force will increase with it.

Unlike the plate, the cylinder's characteristic area remains constant. The average power of the cylinder design, Fig. 5, achieves a greater average power than the single body design for all drag cases. It is also evident that the damped natural frequency decreases with drag, as the optimal mass ratio increases with an increasing drag coefficient.

While the average power of the sphere design, Fig. 6, exceeds the single body power at low drag coefficients, it behaves more like the plate than the cylinder. To increase the mass of the sphere, the characteristic area must also increase, which increases the drag force even greater.

From the regular wave results, it can be concluded that a cylindrical submerged body, where most of the total mass is from the dry mass, is the optimal shape for a two-body wave energy converter. The cylinder, modelled as a bluff body with a drag coefficient of 2, has an equal maximum average power as the sphere with a drag coefficient of 0.5. Future work for modelling a streamlined cylinder can be done to increase the accuracy of the model, as well as increase the power further.

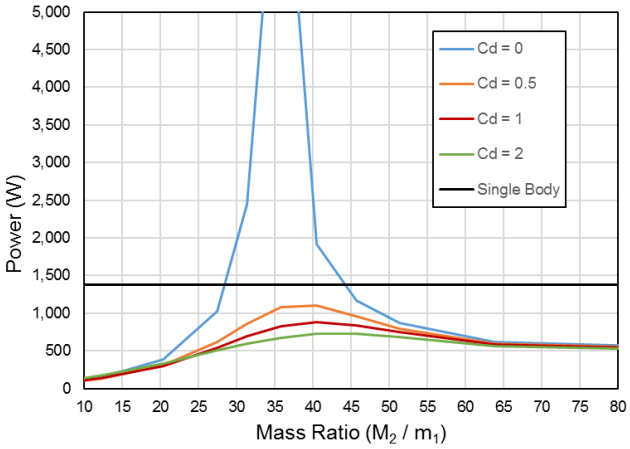

Fig. 4 Regular wave simulations using a plate submerged body

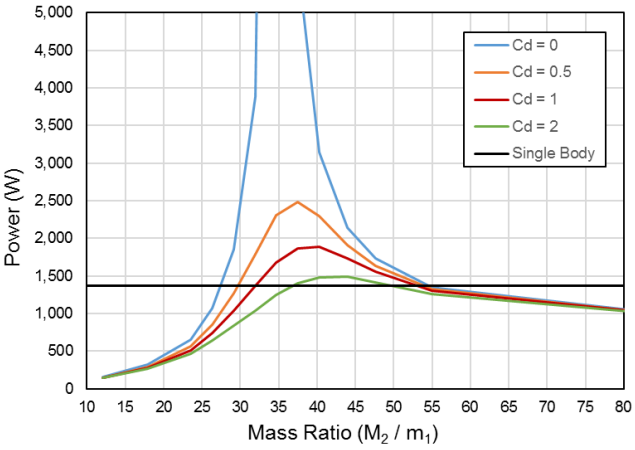

Fig. 5 Regular wave simulations using a cylindrical submerged body

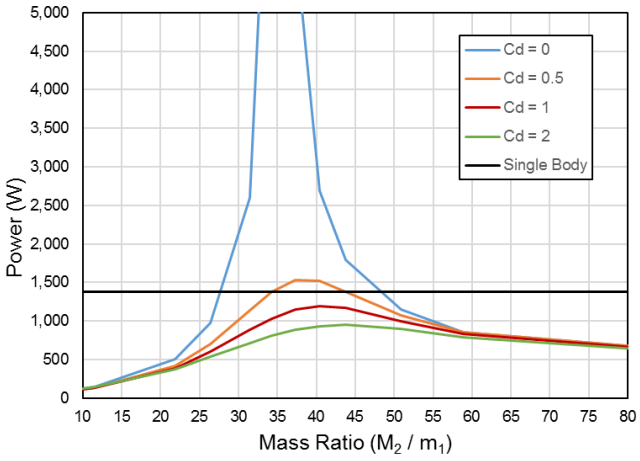

Fig. 6 Regular wave simulations using a spherical plate submerged body

VI. Irregular Waves Results

To see if our conclusion applies to real wave scenarios, irregular wave simulations using a Pierson-Moskowitz spectrum with a peak period and significant wave height of 6s and 1.5m, respectively, were conducted. The case for no drag is not analyzed, as it is not realistic and there is no resonance condition to observe due to the spectrum of the irregular wave.

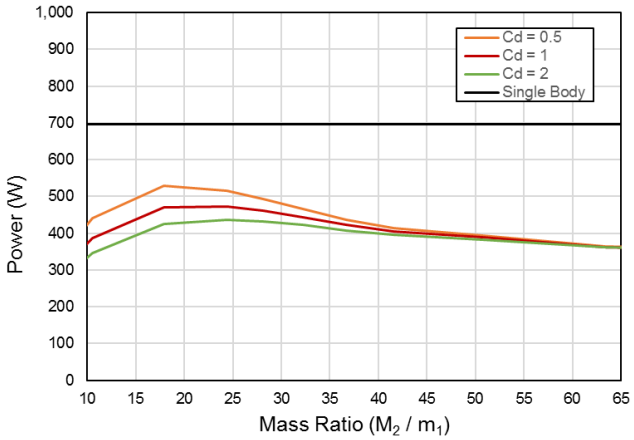

Fig. 7 Irregular wave simulations using a plate submerged body

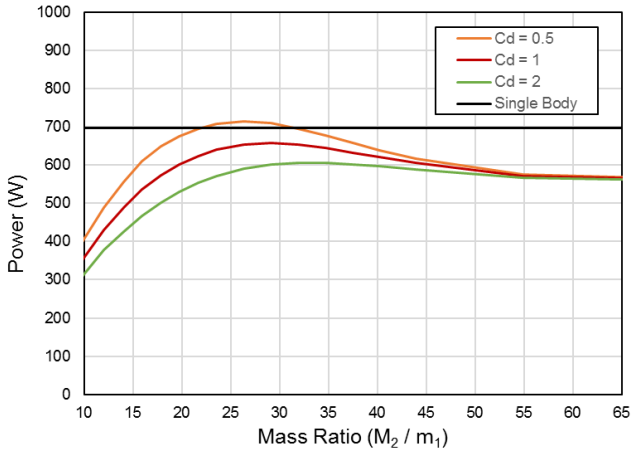

Fig. 8 Irregular wave simulations using a cylindrical submerged body

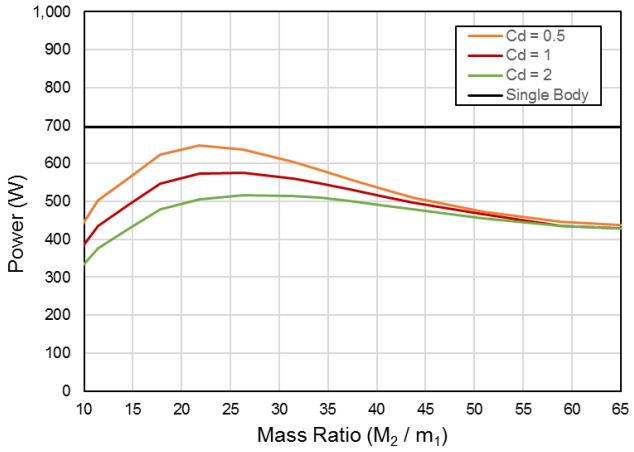

Fig. 9 Irregular wave simulations using a spherical submerged body

While the maximum average power decreases in irregular waves, the same trends that appeared in the regular wave analysis are present. The cylinder design, Fig. 8, has the greatest maximum average power, though it only exceeds the single body power for a drag coefficient of 0.5. The mass ratios are also decreased for irregular wave simulation, the optimal value being in the low to mid 20s.

VII. Conclusion

The shape of the submerged body on a two-body wave energy converter is studied in this paper. For this study, varying shapes and sizes of the submerged body were investigated to see the influence the submerged body has on the absorption power of a two-body system. Three different submerged body shapes were investigated; plate, cylinder and sphere. Simulations were completed for both regular and irregular wave conditions. It was found that the maximum power for each shape will occur at an optimal mass ratio. For the wave energy converter in this paper, the optimal mass ratio in regular waves (period of 6s and wave height of 1.5m) occurs at approximately 35. It is also found that when viscosity is not accounted for, the power of the two-body system will achieve resonance. However, not accounting for viscous effects is unrealistic, as the response of the system becomes unstable. Various drag coefficients were selected to investigate the effect of the drag coefficient on the system response and power absorption. It was found that when viscosity is included in the model, the cylinder design performs the best, exceeding the power of the sphere and plate for all drag cases. To see the performance in real waves, irregular wave simulations using a Pierson-Moskowitz spectrum were completed. While the maximum average power was decreased in irregular waves, the same trends that appeared in the regular wave analysis were present. Again, the cylinder design performed the best. The optimal mass ratios were also decreased to approximately 20 – 25. From these results, it can be concluded that a cylindrical submerged body, where most of the total mass is from the dry mass, is the optimal shape for a two-body wave energy converter. Future work for modelling and designing a streamlined cylinder can be done to further decrease the drag coefficient, which will increase the accuracy of the model, as well as the average absorbed power.

Acknowledgment

We would like to acknowledge the support and funding from the U.S. Department of Energy (DOE) and the National Science Foundation (NSF), as well as our collaborations with the National Renewable Energy Laboratory (NREL).

References

[1] V. Neary, M. Previsic, R. Jepsen, M. Lawson, Y. Yu, A. Copping, A. Fontaine, K. Hallett, and D. Murray. “Methodolgies for Design and Economic Analysis of Marine Energy Conversion (MEC) Technologies,” Sandia National Laboratories, Albuquerque, NM, SAND2014-9040, 2014.

[2] W. Dick, “Wave energy converter,” U.S. Patent 6 857 266, Feb. 22, 2005.

[3] S. Beatty, M. Hall, B. Buckham, P. Wild, and B. Bocking, "Experimental and numerical comparisons of a self-reacting point absorber wave energy converters in regular waves," *Ocean Engineering*, vol. 104, pp. 370–386, Jun. 2015.
[4] (2016) Ocean Power Technologies. [Online]. Available: http://www.oceanpowertechnologies.com
[5] C. Liang and L. Zuo, "On the dynamics and design of a two-body wave energy converter," *Renewable Energy*, vol. 101, pp. 265–274, Feb. 2017.
[6] J. Falnes, "Wave-energy conversion through relative motion between two single-mode oscillating bodies," *ASME OMAE*, vol. 121 pp. 32-38, Feb. 1999.
[7] "Typical data from a field station offshore port of Keelung (nearby NTOU test site)," National Taiwan Ocean University, Keelung, Taiwan.
[8] (2017) WEC-Sim (Wave Energy Converter SIMulator). [Online]. Available: https://wec-sim.github.io/WEC-Sim/index.html
[9] K. Ruehl, C. Michelen, S. Kanner, M. Lawson, and Y. Yu, "Preliminary verification and validation of WEC-Sim, an open-source wave energy converter design tool," in *Proc. OMAE2014*, 2014, paper 24312.
[10] *WAMIT User Manual V7.2*, WAMIT, Inc., 2016.